Liquid-Phase Hydrogenation Kinetics of Multicomponent Aromatic Mixtures on Ni/Al$_2$O$_3$

Mikko S. Lylykangas,* Petri A. Rautanen,[†] and A. Outi I. Krause

Helsinki University of Technology, Department of Chemical Technology, P.O. Box 6100, FIN-02015 HUT Helsinki, Finland.

The hydrogenation reactivity of some aromatic compounds used to model diesel fractions was examined under sulfur-free conditions. Reactions of toluene, 1,2,3,4-tetrahydronaphthalene (tetralin), and naphthalene, separately and as mixtures, were studied using a commercial Ni/Al$_2$O$_3$ catalyst. The reactivity decreased in the following order: naphthalene ≫ tetralin > toluene. Because of competitive adsorption and subsequent inhibition, naphthalene severely reduced the other hydrogenation rates in mixtures, whereas the hydrogenation rate of naphthalene was little affected by the concentration of toluene or tetralin. A kinetic model based on the general form of the Langmuir−Hinshelwood equation was developed. The activation energies of toluene, tetralin, and naphthalene were found to be 52.9, 40.4, and 58.7 kJ/mol, respectively, and the reaction orders of the monoaromatic and diaromatic compounds were about 1.4 and 2.1, respectively. Furthermore, simulations showed that the reaction kinetics in mixtures can be successfully described with models based on single-compound experiments, if surface-concentration terms ($K_i c_i$) for all aromatics are included in the rate equations.

1. Introduction

The oil refinery industry today faces increasing production demands for diesel fuels, at the same time that fuel specifications are being tightened. Intensive research toward more efficient hydroprocessing units is therefore being pursued. Hydroprocessing of diesel consists of the removal of heteroatoms (S, N, O) and aromatic compounds. Aromatic compounds are hydrogenated to saturated hydrocarbons because aromatics have been found to increase both particulate and NO$_x$ emissions from combustion engines.[1,2] Regulations today limit total aromatics contents to 36 wt % in the U.S. and polyaromatics contents to 11 wt % in the EU.[3] Tighter limitations are, however, forthcoming. The World Fuels Charter, issued by engine and vehicle manufacturers, specifies improved qualities for diesel fuel of the future. Among these qualities are total contents of aromatics and polyaromatics as low as 15 and 2 wt %, respectively.[3]

Hydrogenation reactors used in dearomatization are typically co-current downward-flow trickle beds. Supported nickel and platinum are the most commonly applied catalysts. Platinum is superior in activity, but nickel has the advantages of lower price and reaction temperatures. Both catalysts are sensitive to catalyst poisons, mainly sulfur, and the feed to the dearomatization reactor must be purified of these compounds. Hydroprocessing is thus typically performed in two stages. In the first stage, heteroatomic compounds are removed with a sulfided NiMo, CoMo, or NiW catalyst, and in the second stage, the aromatics are hydrogenated with a more active hydrogenation catalyst (nickel or noble metal).[3,4]

Several types of aromatic compounds coexist in diesel fraction. Nevertheless, kinetic experiments have most commonly been done with a single model compound. The corresponding kinetic models are then utilized in process scale-up and optimization. In multicomponent mixtures, the competitive adsorption of aromatics can be expected to affect the hydrogenation rates. Wauquier and Jungers[5] reported already in the 1950s that reactivity depends not only on the rate constant but also on the adsorption coefficient governing the distribution of the catalytic surface among the competing substances. Korre et al.[6] found that both the rates and the adsorption equilibrium constants increase with hydrogenation reactivity in mixtures of mono- and polyaromatic hydrocarbons on a sulfided CoMo/Al$_2$O$_3$ catalyst and that estimated adsorption parameters can be used as a quantitative estimate of the inhibition effect. Toppinen et al.[7] reported a queue effect for the hydrogenation of a multicomponent monoaromatic mixture on Ni/Al$_2$O$_3$ in a semibatch reactor, where only the most reactive component started to hydrogenate immediately and other components did not begin to react until almost complete conversion of the first component had been achieved. The queue effect was also described with kinetic equations based on competitive adsorption of the aromatic substances.

The work of Toppinen et al.[7] looked at the effects of alkyl substituents on the hydrogenation rates of monoaromatic compounds, whereas our study concentrates on the competitive hydrogenation of mixtures of mono- and diaromatic substances, which better describe real diesel fuels. In the experiments, mixtures of toluene, 1,2,3,4-tetrahydronaphthalene (tetralin), and naphthalene were hydrogenated on a commercial Ni/Al$_2$O$_3$ hydrogenation catalyst. Toluene represents the monoaromatics and naphthalene the diaromatics typically present in diesel fractions. Tetralin, which is a partially hydrogenated intermediate of naphthalene, was included to provide

---

* Corresponding author. Fax: +358-9-4512622. E-mail: mikko.lylykangas@hut.fi.
[†] Current address: Nynäs Naphthenics, Oljeraffinaderiet, S-14982 Nynäshamn, Sweden.

information on the successive hydrogenation steps of polyaromatic compounds.

2. Experimental Section

2.1. Apparatus. The experiments were carried out in a three-phase Robinson−Mahoney reactor (50 mL) that was operated in CSTR mode. The reactor was equipped with a fixed catalyst basket and a magnetic stirrer. The feed gas and liquid flows were regulated with mass flow controllers. The reaction pressure was maintained at the desired level by regulating the gas outlet stream. The temperature was adjusted with a programmable temperature controller (±0.5 °C). The product samples were taken through an automatic on-line valve and analyzed quantitatively with a gas chromatograph equipped with a fused silica capillary column and a flame ionization (FI) detector. A more detailed description of the experimental setup can be found elsewhere.[8]

2.2. Catalyst and Chemicals. All experiments were carried out with a commercial nickel/alumina catalyst (16.6 wt % Ni, 108 m^2/g specific surface area, 0.37 cm^3/g mean pore volume). To minimize internal mass- and heat-transfer limitations, industrial-sized pellets were crushed to a particle size of 0.5−0.6 mm. The maximum temperature difference inside the particles was thereby reduced to an insignificant level (<0.5 °C). Preliminary experiments with various particle sizes showed that, for diffusion limitations inside the catalyst to be avoided, even smaller particle sizes would have been required.[8] This was not possible, however, owing to the screen opening in the available catalyst basket, and thus, the internal mass transfer had to be considered in the kinetic modeling.

Before each experiment, the catalyst was dried at 110 °C in nitrogen and then reduced in situ at 400 °C for 2 h in hydrogen flow. The pretreatment procedure was automated to ensure reproducible activity and stability of the catalyst. Hydrogen (99.999%) and nitrogen (99.9999%) were supplied by AGA. Liquid feeds were made up of n-decane (>98%, Fluka), toluene (>99.7%, Riedel-de-Haën), naphthalene (>99%, Acros), and tetralin (>97%, Fluka). All compounds were used as received.

2.3. Kinetic Experiments. Temperature, pressure, and initial concentrations were used as variable reaction parameters. Temperatures varied between 80 and 140 °C in 20 °C intervals, and pressures of 20, 30, and 40 bar were applied. n-Decane was used as a solvent, and the initial molar fractions of the aromatic compounds were 0, 10, or 20 mol % for toluene; 0, 5, or 10 mol % for tetralin; and 0, 3, or 6 mol % for naphthalene. The hydrogen-to-aromatic molar ratio in the feed was thus 4.6−60.

A typical run consisted of five (4−5-h) periods with different combinations of the reaction parameters. In addition, a standard period with reference conditions (20 mol % toluene, 120 °C, 20 bar) was included at the beginning and end of each run to monitor the catalyst activity. After catalyst reduction, experiments were started with liquid and nitrogen flows until the reactor dynamics reached steady state. Thereafter, the reaction was initiated by changing the gas feed to hydrogen, and thus, a precise starting time for the reaction was specified.
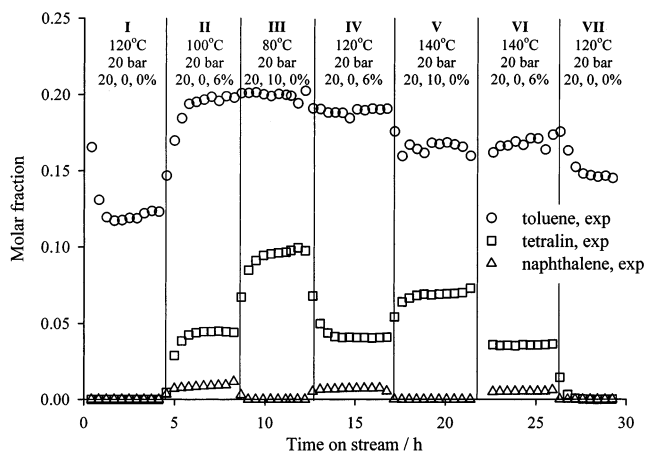
Figure 1. Molar fractions of toluene, tetralin, and naphthalene in experiment A. Temperature, pressure, and feed composition (mol %) in each stage are shown at the top in the order (1) toluene, (2) tetralin, and (3) naphthalene; e.g., the feed of stage II consisted of 20 mol % toluene and 6 mol % naphthalene in n-decane.

3. Results and Discussion

3.1. Qualitative. Unreacted toluene, tetralin, and naphthalene were found in the liquid product streams together with the fully hydrogenated products methyl-cyclohexane and *trans*- and *cis*-decahydronaphthalene (-decalin). In addition, small amounts of $\Delta^{9,10}$-octahydronaphthalene (-octalin) and traces of $\Delta^{1,9}$-octahydronaphthalene (-octalin) were detected. The quantitative determination of $\Delta^{1,9}$-octalin was not possible with the applied methods of analysis, so this isomer was excluded from the further processing of the results. Methylcyclohexane was the only observed hydrogenation product of toluene, whereas tetralin was an intermediate in the hydrogenation of naphthalene, i.e., naphthalene was first hydrogenated to tetralin, which further reacted through $\Delta^{9,10}$- and $\Delta^{1,9}$-octalin to *trans*- and *cis*-decalin. The molar ratio of the trans and cis isomers in the experiments was close to unity, and it was virtually independent of temperature, pressure, or initial concentrations.

Figure 1 depicts the molar fractions of toluene, tetralin, and naphthalene in a typical test run as a function of time on stream. The reaction rates of the model compounds decreased in the following order: naphthalene $\gg$ tetralin > toluene. The order was the same when these compounds were hydrogenated separately.[8−10] The reaction rates were affected by the presence of other aromatic compounds, however. That is, the hydrogenation rates of toluene and tetralin were low when unreacted naphthalene was present in the mixture, whereas the reaction rate of naphthalene to form tetralin was only slightly affected by the concentrations of toluene and tetralin.

The effect of naphthalene on the reaction rate of toluene can be seen in Figure 1 by comparing stages I, IV, and VII, for which the temperature (120 °C), pressure (20 bar), and feed concentration of toluene (20 mol %) were the same. The introduction of 6 mol % naphthalene severely retarded the reaction of toluene in stage IV. This is elucidated in Figure 2, where the average formation rate of methylcyclohexane is plotted for these stages. As can be seen, the rate of hydrogenation of toluene to methylcyclohexane is considerably slower in stage IV, where naphthalene is introduced in

the feed. The fact that the rate is again higher at the end of the experiment (stage VII) confirms that catalyst deactivation alone is not responsible for the decrease in rate from stage I to stage IV.

The explanation for the decrease in the hydrogenation rates of toluene and tetralin in the presence of naphthalene is suggested to be the competitive adsorption of the model compounds and consequent inhibition effect: naphthalene forms strong chemical bonds with nickel and therefore inhibits the chemisorption of toluene and tetralin. In the stages where the conversion of naphthalene was close to complete, the rates for toluene and tetralin hydrogenation were again higher. This is consistent with reported data, according to which the saturated hydrogenation products are not as strongly bonded on the surface as their aromatic analogues.[11] This means that toluene and tetralin are able to adsorb on the catalyst and react at high conversion levels of naphthalene.

Standard periods at the beginning and end of the experiments showed that the catalyst activity dropped to about 70% of its original value during the run. Deactivation, which followed approximately a first-order rate equation and was only weakly dependent on temperature, was assumed to be due to the formation of hydrogen-deficient species. The benzene ring is known to chemisorb through π-bonds with its ring parallel to the metal surface. The π-bonded compounds can lose hydrogen and form less reactive σ-bonded surface species. Further dissociation of these surface compounds leads to the formation of coke and the loss of active metal surface.[12,13] Earlier experiments with single model compounds[9,10] support this assumption: the deactivation rate was an order of magnitude higher when tetralin was hydrogenated (high tetralin concentration) than when naphthalene was hydrogenated (tetralin as an intermediate). This finding is consistent with observations according to which aliphatic C–H bonds (present in tetralin but not in naphthalene) are more easily dissociated than the corresponding aromatic bonds.[14]

Reproducibility of the experimental data was examined by comparing the formation rates of methylcyclohexane in the first standard period of each experiment (120 °C, 20 bar, 20 mol % of toluene in n-decane). These duplicates showed that the experiments were rather well reproducible: the maximum variation in the rates was ±7% from the average. This variation was assumed to be due to inhomogenieties in the catalyst, and it was eliminated in the kinetic modeling by normalizing the experiments, i.e., multiplying the catalyst mass of each experiment by a correction factor so that the rates in the standard periods of the experiments were equal. The accuracy of the compositional analysis was evaluated by calculating the mass balances for the aromatics and their hydrogenation products. These evaluations verified that the applied analysis method was accurate and reproducible and showed that the largest relative errors (5%) were associated with low aromatic feed contents.

3.2. Model for the Hydrogenation Kinetics. The mechanism of stepwise hydrogen addition was supported by our results, namely, the formation of partly hydrogenated intermediates (octahydronaphthalenes) in tetralin hydrogenation and the formation of tetralin at low naphthalene conversions. No traces of methylcyclohexenes, as intermediates in the hydrogenation of
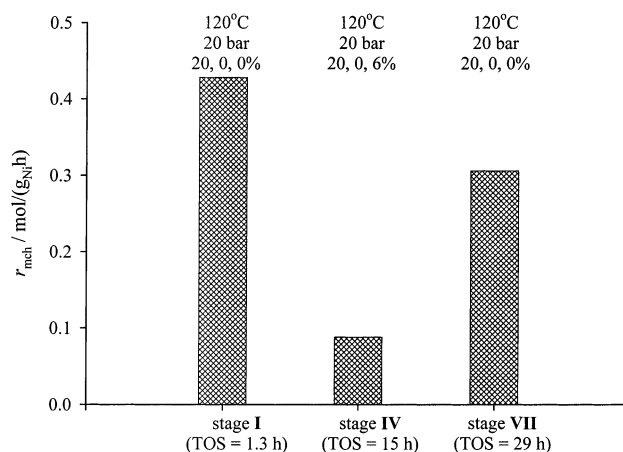
Figure 2. Formation rates of methylcyclohexane in experiment A. Temperature, pressure, and feed composition (mol %) in each stage are shown at the top in the order (1) toluene, (2) tetralin, and (3) naphthalene; e.g., the feed of stage IV consisted of 20 mol % toluene and 6 mol % naphthalene in n-decane.

toluene, were found, perhaps because of kinetic coupling, i.e., the high reactivity of these intermediates relative to toluene under the applied reaction conditions.

The net reactions of toluene to methylcyclohexane and naphthalene to tetralin were straightforward, each giving only one product with a saturated ring. The reaction scheme for the hydrogenation of tetralin was more complicated. The reaction mechanism, including the stereochemistry and selectivities to *cis*- and *trans*-decalin, has been presented in detail in a previous paper.[9] The scheme was simplified in the present study to reduce the number of kinetic parameters. Because the molar fraction of octalins was low in each experiment, these components were lumped together with decalins in the parameter estimation. Furthermore, thermodynamic calculations with the FLOWBAT program[15] showed that none of the hydrogenation reactions was equilibrium-limited under the studied conditions: the calculated equilibrium constants were 8.3×10^{10}–4.6×10^{15}, 4.8×10^6–3.5×10^9, and 7.0×10^8–2.7×10^{13} for toluene, naphthalene, and tetralin hydrogenation, respectively. Indeed, equilibrium limitations in naphthalene hydrogenation would have appeared only if reaction temperatures above 320 °C had been applied (equilibrium constant value below 10). Thus, all of the reactions can be treated as irreversible, and the reaction system can be represented as follows

(1)

(2)

(3)
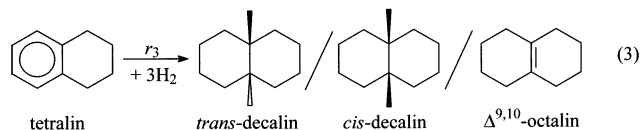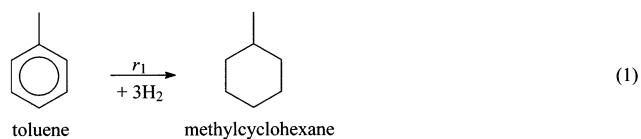
The net reaction rates for the components can be written as follows

$$r_{\text{toluene}} = -r_1 \tag{4}$$

$$r_{\text{naphthalene}} = -r_2 \tag{5}$$

$$r_{\text{tetralin}} = +r_2 - r_3 \tag{6}$$

$$r_{\text{mch}} = +r_1 \tag{7}$$

$$r_{\text{oct+dec}} = +r_3 \tag{8}$$

$$r_{\text{hydrogen}} = -3r_1 - 2r_2 - 3r_3 \tag{9}$$

It is assumed in eqs 3 and 9 that three hydrogen molecules are consumed in the reactions of tetralin. This is not true for the reaction of tetralin to form $\Delta^{9,10}$-octalin, where only two molecules are inserted into the aromatic ring. The molar fraction of $\Delta^{9,10}$-octalin in the experiments was low (<0.5%), however, and the error in the hydrogen consumption rate (eq 9) can be considered negligible.

The general form of the Langmuir–Hinshelwood equation[16] was chosen as the basis for the kinetic equations for the stoichiometric eqs 1–3. The general form was simplified by assuming the same reaction orders for the two monoaromatic compounds, because the preliminary estimations had shown that the reaction orders with respect to toluene and tetralin were virtually the same. Furthermore, the same reaction order for hydrogen in each of the reactions 1–3 was assumed. The additional assumption of competitive adsorption leads to the equation

$$-r_i = \frac{k_i c_i^{m_i} c_{\text{H}_2}^{m_{\text{H}}}}{[1 + (K_{\text{H}} c_{\text{H}})^{1/\gamma} + \sum_j K_j c_j]^{1+\gamma}} \tag{10}$$

The term γ was set floating so that an indication of the chemical nature of the active hydrogen in the reactions could be obtained. The estimated values $\gamma = 1$ and $\gamma = 2$ would then indicate hydrogen taking part in the reactions in the molecular and dissociative forms, respectively. The summation term in the denominator includes only the aromatic hydrocarbons because the adsorption of saturated compounds on metal catalysts is considerably weaker.[17] The use of liquid-phase hydrogen concentrations instead of gas-phase hydrogen partial pressures enables the direct applicability of the rate expressions in reactor design. Hydrogen solubility values were estimated using the Soave–Redlich–Kwong equation of state. Figure 3 depicts the calculated hydrogen solubility values in pure solvent (n-decane) and in a typical reaction mixture (10 mol % toluene, 5 mol % tetralin, and 3 mol % naphthalene in n-decane) at different temperatures and pressures. The graphs show that the molar fraction of hydrogen increases as a function of temperature and pressure but decreases as a function of aromatic content.

The temperature dependency of the rate constants was modeled with the Arrhenius equation

$$k_i(T) = k_{i,\text{ref}} \exp\left[-\frac{E_a}{R}\left(\frac{1}{T} - \frac{1}{T_{\text{ref}}}\right)\right] \tag{11}$$
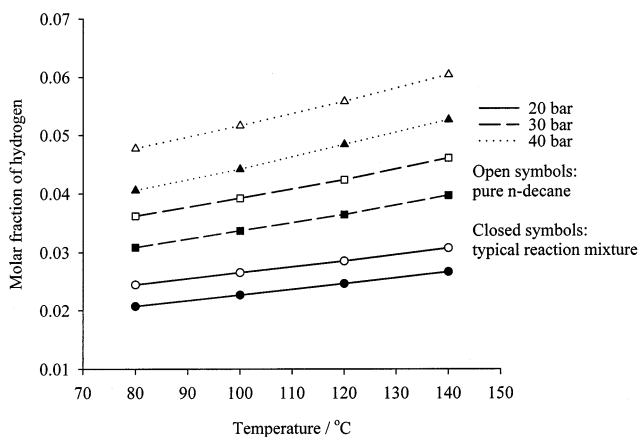
Figure 3. Hydrogen solubility values in pure solvent (n-decane) and in typical reaction mixture (10 mol % toluene, 5 mol % tetralin, and 3 mol % naphthalene in n-decane) at different temperatures and pressures according to the Soave–Redlich–Kwong equation of state.

($T_{\text{ref}} = 110$ °C), whereas the adsorption equilibrium constants were assumed to be independent of temperature. Usually, the temperature dependency of K_j is described with the law of van't Hoff. However, as originally reported by Temkin[18] and experimentally confirmed by Babernics et al.,[19] the heat of adsorption decreases as the surface coverage increases. The concentrations and surface coverages are typically large in the liquid phase, and the effect of temperature on adsorption was therefore assumed to be negligible in the temperature interval studied.

3.3. Reactor Model. The dynamic reactor model consisted of material balances in the gas and liquid phases for all compounds present in the reaction mixtures

$$\frac{dn_i^{\text{G}}}{dt} = F_{\text{in},i}^{\text{G}} - V_R N_{\text{GL},i} a_{\text{GL}} - F_{\text{out},i}^{\text{G}} \tag{12}$$

and

$$\frac{dn_i^{\text{L}}}{dt} = F_{\text{in},i}^{\text{L}} + V_R N_{\text{GL},i} a_{\text{GL}} + V_R N_{\text{LS},i} a_{\text{LS}} - F_{\text{out},i}^{\text{L}} \tag{13}$$

where V_R is the volume of the reactor (50 mL) and $N_{\text{GL},i} a_{\text{GL}}$ and $N_{\text{LS},i} a_{\text{LS}}$ are the mass-transfer rates of component i at the gas–liquid and solid–liquid interfaces, respectively. The mass-transfer rates between gas and liquid phases, $N_{\text{GL},i} a_{\text{GL}}$, were estimated by the two-film theory. Because it was verified in earlier experiments[8] that gas–liquid mass transfer did not have an effect on the overall rates, high values were assigned to the mass-transfer coefficients ($\kappa_{\text{L}} a_{\text{GL}} = 1.0 \times 10^2$ s^{-1} and $\kappa_{\text{G}} a_{\text{GL}} = 1.0 \times 10^4$ s^{-1}). The reactor dynamics was studied with step response experiments, and the experiments verified that the reactor could be treated as an ideal CSTR. According to the step responses, the volume of the liquid phase was 28.6 mL at steady state, and thus, the volume of the gas phase was obtained as (50 − 28.6) mL = 21.4 mL. Hydrogen solubilities were calculated with the Soave–Redlich–Kwong equation of state, which Parks et al.[20] have shown to be an accurate method for estimating properties of mixtures of hydrogen and aromatics.

The mass-transfer limitations inside the catalyst particles could not be eliminated in the experiments, and component balances inside catalyst particles were written assuming spherical geometry. Average values for aluminum oxide were used as the values for the constriction factor and tortuosity: $\epsilon_p = 0.50$, $\tau_p = 4.0$.[21] Molecular diffusion coefficients were calculated with the Wilke–Chang equation, which is an old but still widely used correlation for binary diffusion coefficients. For a wide range of solute–solvent systems, an average error of about 10% has been reported for this correlation.[22] Owing to external heating and cooling, energy balances for the bulk phases were not needed. Furthermore, the energy balance for the particle was omitted, because a calculation according to the equation

$$(\Delta T)_{\text{max}} = \frac{\sum_i [c_i(-\Delta H_{\text{R},i})D_{\text{eff},i}]}{k_t} \qquad (14)$$

had shown that, under the applied conditions, the maximum temperature difference inside the catalyst particles was less than 0.5 °C.

Component balances inside the catalyst particle (PDE) were discretized by a 5-point central difference formula in 12 pieces with a logarithmic grid. The fluxes between the porous catalyst particle and the liquid phase (apparent reaction rates), $N_{\text{LS},i}$, were then calculated for the liquid phase mole balance (eq 13) by summing up the average rates in each discretization piece. Thereafter, the linear system of ordinary differential eqs 12 and 13 was integrated numerically by the backward difference method.[23]

Catalyst deactivation was assumed to be due to coking. However, no methods were available for the quantitative analysis of coke content on the catalyst during the experiments. Because the implementation of a concentration-dependent deactivation model would have led to coupling between the deactivation and kinetic parameters and because the activity loss was approximately the same in all experiments, an empirical power-law equation was applied in the modeling of deactivation

$$-\frac{\text{d}a}{\text{d}t} = k_d a^d \qquad (15)$$

Temperature did not have a significant effect on the deactivation rate, and the temperature dependency of the coefficient k_d was therefore neglected.

3.4. Parameter Estimation. Parameter estimation was done simultaneously with the numerical integration of the reactor model eqs 12 and 13. The objective function was the sum of squares of the errors between the experimental and calculated molar fractions in liquid products

$$\text{RSS} = \sum_i (x_{i,\text{exp}} - x_{i,\text{calc}})^2 \qquad (16)$$

Minimization was carried out with the in-house optimization program KINFIT utilizing the Levenberg–Marquardt method. An absolute least-squares objective function was chosen instead of a relative function, because the relative error increased as the molar

Table 1. Estimated Kinetic Parameters with 95% Confidence Intervals[a]

	$k_{i,\text{ref}} \times 10^5$ $\left[\dfrac{\text{mol}}{g_{\text{Ni}}\,\text{h}}\left(\dfrac{\text{m}^3}{\text{mol}}\right)^{m_i+m_H}\right]$	$E_{a,i}$ (kJ/mol)	$K_i \times 10^3$ (m^3/mol)	m_i
toluene	0.30 ± 0.09	52.9 ± 1.7	1.0 ± 0.2	1.43 ± 0.04^b
naphthalene	12.2 ± 9.5	58.7 ± 8.6	7.8 ± 2.5	2.1 ± 0.2
tetralin	0.91 ± 0.24	40.4 ± 1.3	4.4 ± 1.0	1.43 ± 0.04^b
hydrogen	–	–	3.7 ± 3.0	1.0 ± 0.1^c

^{a} $\gamma = 1.8 \pm 0.3$. ^{b} Same reaction order was assumed for toluene and tetralin ^{c} Same reaction order for hydrogen in each of the reactions.

fractions of the aromatics and their products became smaller, so that estimations with the relative least-squares objective function gave dubious results.

The empirical deactivation parameters k_d and d had values of $8.7 \pm 1.6 \times 10^{-6}$ s^{-1} and 0.87 ± 0.37, respectively. The deactivation rate and order are close to those estimated in our earlier experiments with tetralin[9] ($d = 1.19 \pm 0.05$) but substantially different from those estimated in experiments with naphthalene.[10] For naphthalene, deactivation was slower and followed a nearly zeroth-order equation. This difference is consistent with the assumption that the catalyst deactivation is mainly due to the aliphatic groups of the model compounds.

The estimated kinetic parameters with 95% confidence intervals are presented in Table 1. The activation energies for toluene, naphthalene, and tetralin are 52.9, 58.7, and 40.4 kJ/mol, respectively. The values for the monoaromatics are well in accordance with those reported for gas- and liquid-phase hydrogenations,[24–26] whereas no reported values for the activation energy of naphthalene hydrogenation on nickel were found in the literature. The estimated reaction rate constants and adsorption equilibrium constants decrease in the order naphthalene > tetralin > toluene, which is consistent with the qualitative observations. Adsorption equilibrium constants for naphthalene and tetralin are of the same order of magnitude as in our previous study with naphthalene as a model compound.[10] In that study, the temperature dependency of the adsorption parameters was modeled according to the van't Hoff equation. At the average temperature (110 °C), the values were 5.2×10^{-3} for naphthalene and 3.2×10^{-3} for tetralin, compared with the values of 7.8×10^{-3} (naphthalene) and 4.4×10^{-3} (tetralin) in this study. The estimated value of 1.8 for the parameter γ is also consistent with our earlier experiments[10] and indicates that chemisorbed H atoms could be the active hydrogen species in the reactions rather than molecular hydrogen.

The term $(K_H c_H)^{1/\gamma}$, which describes the surface concentration of hydrogen, is the smallest term in the denominator of the rate eq 10. This implies low coverage of active hydrogen compared to the aromatics on the catalyst surface. Under these conditions, dissociation of C–H bonds and consequent formation of hydrogen-deficient species could, indeed, explain catalyst deactivation.

The confidence intervals are largest for the parameters of naphthalene, because of its high reactivity and thus low concentrations in product streams. However, the model describes all reactions with adequate accuracy (Figure 4). Values of the residual sum of squares and residual root-mean-square errors for the 1219 data points are 0.18 and 5.0×10^{-3}, respectively.
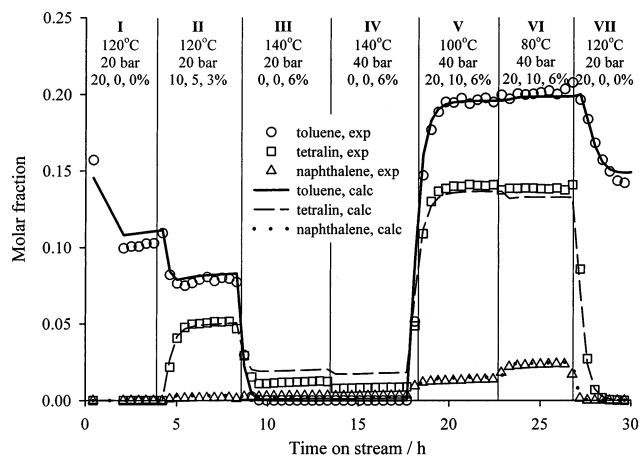
Figure 4. Experimental and calculated molar fractions of toluene, tetralin, and naphthalene in experiment B. Feed composition (mol %) in each stage is shown at the top in the order (1) toluene, (2) tetralin, and (3) naphthalene.

Internal diffusion limited the overall rates even at the lowest reaction temperature. At 80 °C and 20 bar, typical values of the Weisz–Prater criterion based on the toluene, tetralin, and naphthalene consumptions were 1.3, 0.7, and 3.1, respectively, and at 120 °C and 20 bar, the corresponding values were 6.5, 2.0, and 9.8, respectively. The internal mass-transfer limitation was less severe with mixtures than with pure reactants as a result of the inhibition effect. Figure 5 depicts the concentration profiles as a function of the dimensionless

radius (λ) at 80 and 140 °C at 20 bar. The values of 0 and 1 for λ refer to the center and the outer surface of the catalyst particle, respectively. The effect of competitive adsorption is most clearly seen in the shapes of the tetralin profiles. At 80 °C (bottom left), naphthalene inhibits the reaction of tetralin to the saturated products, and the tetralin concentration increases toward the center of the particle. However, at 140 °C (bottom right), the molar fraction of naphthalene drops more steeply toward the center of the particle, enabling a higher reaction rate of tetralin to saturated products. Thus, the tetralin concentration passes through a maximum in the vicinity of the outer surface of the particle.

3.5. Comparison with the Single-Model-Compound Kinetics. The effect of competitive adsorption brings about difficulties in the scale-up and optimization of dearomatization reactors (trickle beds) because compounds with different reactivities form reaction fronts in the axial direction of the catalyst bed. This means that it is not possible to simulate the dearomatization reactor straightforwardly by estimating kinetic parameters only for the least reactive component; rather, the interactions between different aromatic compounds need to be considered as well. In the present study, we wanted to examine whether this can be done by applying kinetic equations from single-compound experiments and taking the interactions into consideration with the competitive adsorption terms in the denominator of the rate equations.
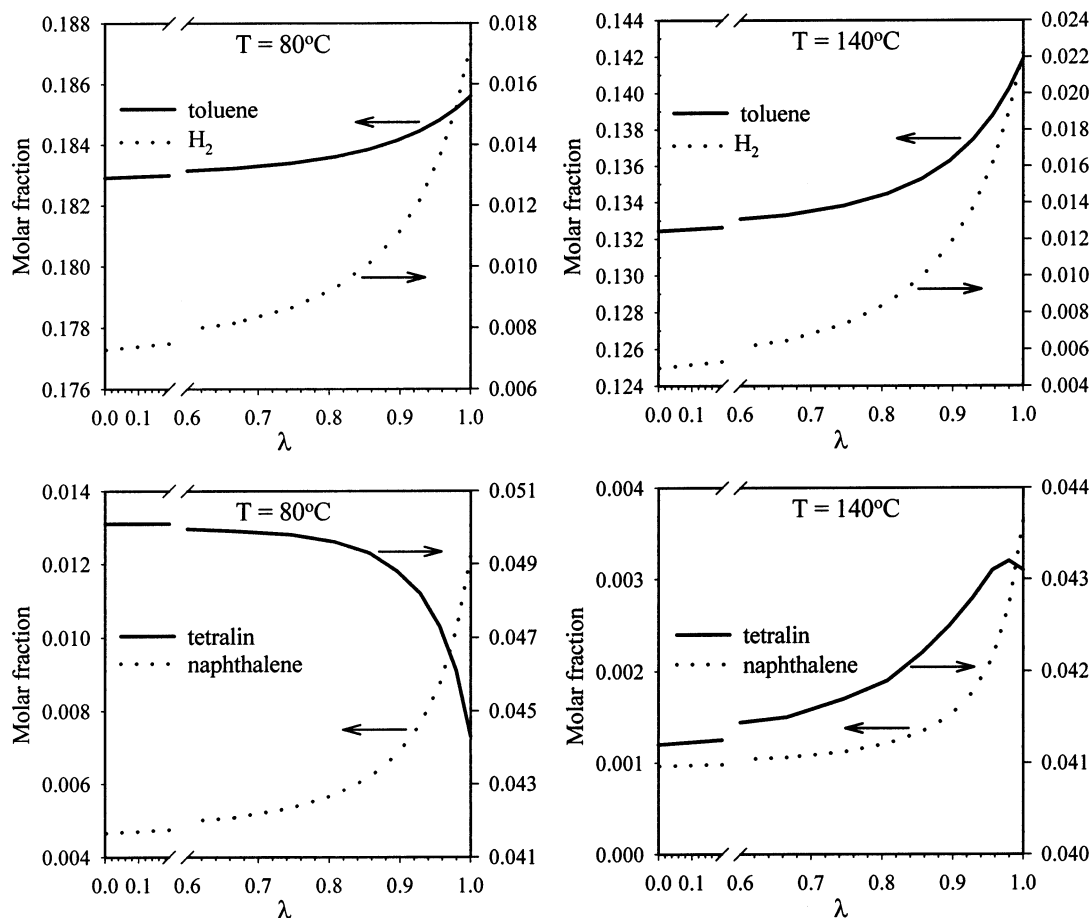
Figure 5. Concentration profiles inside catalyst particles at 80 and 140 °C and at 20 bar hydrogen pressure. Initial composition of the reaction mixture: 20 mol % toluene and 6 mol % naphthalene. Values $\lambda = 0$ and $\lambda = 1$ refer to the center and the outer surface of the catalyst particle, respectively.
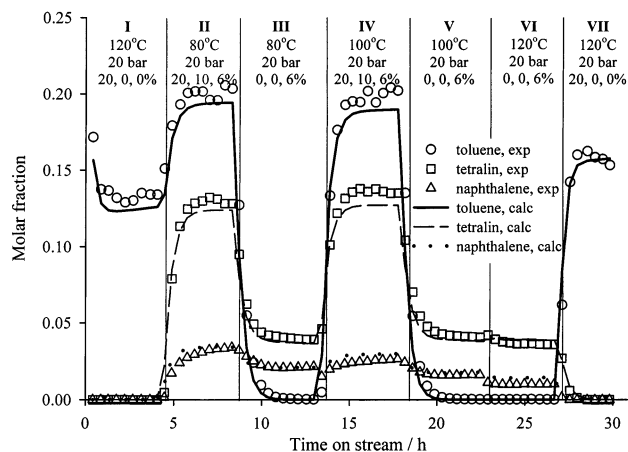
Figure 6. Experimental and calculated molar fractions of toluene, tetralin, and naphthalene in experiment C. Calculated values are based on models developed from single-compound experiments.[8,10] Feed composition (mol %) in each stage is shown at the top in the order (1) toluene, (2) tetralin, and (3) naphthalene.

For this purpose, the present data set was simulated using the kinetic equations and parameter values developed in our earlier work with single model compounds.[8,10] The surface-concentration terms, $K_i c_i$, for the aromatics were summed in the denominator of the rate equations. In Figure 6, the experimental molar fractions of toluene, tetralin, and naphthalene are depicted together with the calculated values in a typical experiment. As can be seen, the product compositions in the mixtures can be predicted rather accurately with kinetic models estimated from experiments with single model compounds. Thus, these models are also applicable in the optimization of dearomatization reactors. However, in the parameter estimation, it is important that excess correlation between parameters be avoided, so that all parameters, especially adsorption equilibrium constants, will have physically meaningful values.

4. Conclusions

The hydrogenation kinetics of mixtures consisting of the model compounds toluene, tetralin, and naphthalene in *n*-decane was studied. The hydrogenation rates of these compounds differ when the compounds are hydrogenated as a mixture and separately: the most reactive component, naphthalene, strongly retards the reactions of toluene and tetralin. We proposed that this was due to the competitive adsorption of the aromatics and to stronger chemical bonding between the catalyst surface and naphthalene.

The formation of partly hydrogenated products in tetralin hydrogenation supported the stepwise hydrogen-addition mechanism. We proposed a semiempirical kinetic model that accounts for the competitive adsorption through $K_i c_i$ terms in the denominator of the rate equations. The model describes the kinetic behavior of the mixtures accurately, and the order of magnitude of the estimated parameters is physically meaningful. In addition, simulations showed that hydrogenation kinetics in aromatic mixtures can be described with rate equations based on single-compound experiments if the adsorption equilibria of all aromatics are included in the rate equations. Single-compound models can therefore be extended and applied in the simulation of hydrogenation reactions in real diesel fractions.

Nomenclature

a = catalyst activity
a_{GL} = gas−liquid mass-transfer area per unit reactor volume, m^{-1}
c_i = concentration of component i, mol/m^3
CSTR = continuous stirred tank reactor
d = deactivation order
D_{eff} = effective diffusion constant, m^2/s
E_a = apparent activation energy, kJ/mol
F = molar flow, mol/s
ΔH_R = reaction enthalpy, J/mol
k = rate constant, units depend on the rate equation
K = adsorption equilibrium constant, mol/m^3
k_d = deactivation coefficient, s^{-1}
k_t = thermal conductivity of the catalyst particle, W/(m K)
m_i = reaction order of component i
n_i = amount of component i in the reactor, mol
$N_{GL,i}$ = flux of component i at the gas−liquid interface, mol/(m^2 s)
$N_{LS,i}$ = flux of component i at the liquid−solid interface, mol/(m^2 s)
r = reaction rate, mol/(g$_{Ni}$ h)
R = universal gas constant [≡8.3144 J/(mol K)]
RSS = residual sum of squares (objective function in eq 16)
t = time, s
T = temperature, K
TOS = time on stream, h
V_R = reactor volume, mL
x = molar fraction in the liquid phase

Sub- and Superscripts

calc = calculated
eff = effective
exp = experimental
G = gas-phase
L = liquid-phase
p = catalyst particle
ref = reference temperature in the parameter estimation (≡110 °C)

Greek Letters

ϵ = porosity of the catalyst
γ = active site occupied by a hydrogen molecule, parameter in eq 10
κ = mass-transfer coefficient, m/s
λ = dimensionless position in the catalyst particle
τ = tortuosity of the catalyst

Literature Cited

(1) Karonis, D.; Lois, E.; Stournas, S.; Zannikos, F. Correlations of Exhaust Emissions from a Diesel Engine with Diesel Fuel Properties. *Energy Fuels* **1998**, *12*, 230.

(2) Kidoguchi, Y.; Yang, C.; Kato, R.; Miwa, K. Effects of Fuel Cetane Number and Aromatics on Combustion Process and Emissions of a Direct-Injection Diesel Engine. *JSAE Rev.* **2000**, *21*, 469.

(3) Hunter, M.; Gentry, A.; Lee, S.; Groeneveld, L.; Olivier, C.; Pappal, D. MAKFining—Premium Distillates Technology: The Future of Distillate Upgrading. Presented at the NPRA 2000 Annual Meeting, San Antonio, TX, Mar 26−28, 2000; Paper AM-00-18.

(4) Cooper, B. H.; Donnis, B. B. L. Aromatic Saturation of Distillates: An Overview. *Appl. Catal. A: Gen.* **1996**, *137*, 203.

(5) Wauquier; J.-P.; Jungers, J. C. Joint Reactions for Comparison of Kinetic Constants in Heterogeneous Catalysis. *Compt. Rend.* **1956**, *243*, 1766.

(6) Korre, S. C.; Klein, M. T.; Quann, R. J. Polynuclear Aromatic Hydrocarbons Hydrogenation. 1. Experimental Reaction Pathways and Kinetics. *Ind. Eng. Chem. Res.* **1995**, *34*, 101.

(7) Toppinen, S.; Salmi, T.; Rantakylä T.-K.; Aittamaa, J. R. Liquid-Phase Hydrogenation Kinetics of Aromatic Hydrocarbon Mixtures. *Ind. Eng. Chem. Res.* **1996**, *36*, 2101.

(8) Rautanen, P. A.; Aittamaa, J. R.; Krause, A. O. I. Solvent Effect in Liquid-Phase Hydrogenation of Toluene. *Ind. Eng. Chem. Res.* **2000**, *39*, 4032.

(9) Rautanen, P. A.; Aittamaa, J. R.; Krause, A. O. I. Liquid-Phase Hydrogenation of Tetralin on Ni/Al$_2$O$_3$. *Chem. Eng. Sci.* **2001**, *56*, 1247.

(10) Rautanen, P. A.; Lylykangas, M. S.; Aittamaa, J. R.; Krause, A. O. I. Liquid-Phase Hydrogenation of Naphthalene on Ni/Al$_2$O$_3$. *Stud. Surf. Sci. Catal.* **2001**, *133*, 309.

(11) Keane, M. A. The Hydrogenation of *o*-, *m*-, and *p*-Xylene over Ni/SiO$_2$. *J. Catal.* **1997**, *166*, 347.

(12) Tjandra, S.; Zaera, F. A Surface Science Study of the Hydrogenation and Dehydrogenation Steps in the Interconversion of C$_6$ Cyclic Hydrocarbons on Ni(100). *J. Catal.* **1996**, *164*, 82.

(13) Lehwald, S.; Ibach, H.; Demuth, J. E. Vibration Spectroscopy of Benzene Adsorbed on Pt(111) and Ni(111). *Surf. Sci.* **1978**, *78*, 577.

(14) Friend, C. M.; Muetterties, E. L. Coordination Chemistry of Metal Surfaces. 3. Benzene and Toluene Interactions with Nickel Surfaces. *J. Am. Chem. Soc.* **1981**, *103*, 773.

(15) Aittamaa, J. R.; Keskinen, K. I. *Flowbat—User's Instruction Manual*; Laboratory of Chemical Engineering, Helsinki University of Technology, Helsinki, Finland, 2000.

(16) Kiperman, S. L. Some Problems of Chemical Kinetics in Heterogeneous Hydrogenation Catalysis. *Stud. Surf. Sci. Catal.* **1986**, *27*, 1.

(17) Huang, T.-C.; Kang, B. C. Kinetic Study of Naphthalene Hydrogenation over Pt/Al$_2$O$_3$ Catalyst. *Ind. Eng. Chem. Res.* **1995**, *34*, 1140.

(18) Temkin, M. I. The Kinetics of Some Industrial Heterogeneous Catalytic Reactions. *Adv. Catal.* **1979**, *28*, 173.

(19) Babernics, L.; Tétényi, P.; Kertész, L. Investigation of the Adsorption of Benzene and Cyclohexane on Some Transition Metals and their Oxides. *Z. Phys. Chem.* **1974**, *89*, 237.

(20) Park, J.; Robinson, R. L., Jr; Gasem, K. A. M. Solubilities of Hydrogen in Aromatic Hydrocarbons from 323 to 433 K and Pressures to 21.7 MPa. *J. Chem. Eng. Data* **1996**, *41*, 70.

(21) Satterfield, C. *Mass Transfer in Heterogeneous Catalysis*; MIT Press: Cambridge, MA, 1970.

(22) Reid, R.; Prausnitz, J.; Poling, P. *The Properties of Gases and Liquids*; McGraw-Hill: New York, 1987.

(23) Hindmarsh, A. C. ODEPACK, A Systematized Collection of ODE Solvers. In *Scientific Computing*; Stepleman, R. S. Carver, M., Peskin, R., Ames, W. F., Vichnevetsky, R., Eds.; IMACSVS/North-Holland: Amsterdam, 1983.

(24) van Meerten, R. Z. C.; Coenen J. W. E. Gas-Phase Hydrogenation on a Nickel-Silica Catalyst IV. Rate Equations and Curve Fitting. *J. Catal.* **1977**, *46*, 13.

(25) Toppinen, S.; Rantakylä, T.-K.; Salmi, T.; Aittamaa, J. Kinetics of the Liquid-Phase Hydrogenation of Bezene and Some Monosubstituted Alkylbenzenes over a Nickel Catalyst. *Ind. Eng. Chem. Res.* **1996**, *35*, 1824.

(26) Cooper, B. H.; Donnis, B. B. L. Aromatic Saturation of Distillates: An Overview. *Appl. Catal. A: Gen.* **1996**, *137*, 203.